Control of Real and Reactive Power using a Novel SVC Feedback System for Load Sharing in Grid Connected PV Power System

Md. Habib Ullah*‡, S.M. Ehsanul Haque**

* Department of Electrical and Electronic Engineering, Ahsanullah University of Science and Technology, Tejgaon, Bangladesh.

** Department of Electronic Engineering, La Trobe University, Melbourne, Australia.

(imshouruv@gmail.com; ehsanulhaque167@gmail.com)

‡ Corresponding Author; Md. Habib Ullah, Department of Electrical and Electronic Engineering, Ahsanullah University of Science and Technology, 141-142 Love Road, Tejgaon, Dhaka-1208, Bangladesh, Email: imshouruv@gmail.com

Received: 22.08.2013 Accepted: 13.10.2013

Abstract- In a power system of conventional parallel-connected generators, share of real power and reactive var of an incoming generator are controlled by adjusting shaft power input and field excitation. The scenario of load sharing by a grid connected PV system is however different. Since no prime mover or excitation source are present. Due to serious power crisis, there is a need for the transfer of PV power to the grid systems. However, this needs intensive analysis on the load sharing phenomena. In this study, aspects of load sharing of a grid connected PV system utilizing boost inverter are analyzed, and a strategy is proposed where the load sharing task can be undertaken controlling the modulation index of the boost inverter. We also have briefly surveyed the characteristics of the boost inverter for different voltage levels and prescribed a range of modulation index for which the system can perform perfectly for each of these voltage levels. It is seen that both real power and reactive var are affected upon the change in the modulation index of the boost inverter. Analysis and simulation results are presented to demonstrate effectiveness of the proposed control technique using boost inverter.

Keywords- Boost inverter, PV system, Static Var Compensator(SVC), Modulation index, SPWM bridge inverter.

1. Introduction

In today's world, electricity is a vital ingredient for both economic and social development. Adequate, reliable and reasonably priced supply of electricity is an essential pre-requisite for national development. Due to the growing energy consumption around the world and the eminent exhaustion of fossil-fuel reserves, a great interest on alternative energy sources can be noticed nowadays. Among the clean and green power sources, the photovoltaic (PV) solar energy comes up as being a very interesting alternative to supplement the generation of electricity [1]. Solar Cells supply electric energy renewable from primary resources. Solar cells are rarely used individually. Cells with similar characteristics are under peak sunlight (1 W/m^2) the maximum current delivered by a cell is approximately 30 (mA/cm^2). Cells are therefore, paralleled to obtain the desired current [5]. So, it can charge a battery up to 12 volt DC. For residential use, all equipments require a pure sinusoidal 220V ac power supply. For this a static DC-AC converter is inserted between the solar cells and the distribution network. DC to AC conversion has been established as one of the most common operations in power electronics [2]. One of the characteristics of the most classical inverter is that it produces an AC output instantaneous voltage always lower than the DC input voltage [4]. Boost DC-AC inverter is a novel converter, whose main advantage is to achieve an output

voltage higher or lower than the input one. Other advantages are the quality of output voltage sine wave and reduced number of switches i.e. only four switches required. This property is not found in the traditional full bridge inverter, which produces an instantaneous ac output voltage always lower than the input dc voltage [3].

2. Equivalent Circuit Diagram of PV Cell

The simplest model of a PV cell is shown as an equivalent circuit below that consists of an ideal current source in parallel with an ideal diode. The current source represents the current generated by photons and its output is constant under constant temperature and constant incident radiation of light.

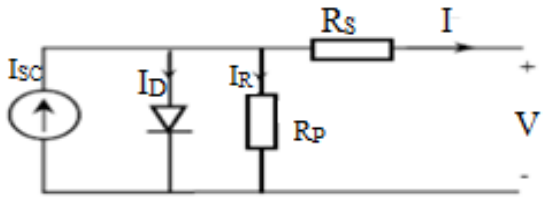

Fig. 1. quivalent electrical circuit of a solar cell.

The I-V characteristics of the equivalent solar cell circuit can be determined by following equations [13]. The current through diode is given by,

$$I_D = I_o\left[e^{\left(\frac{q(V+IR_S)}{nKT}\right)} - 1\right]$$

While, the solar cell output current,

$$I = I_{SC} - I_D - I_R$$

Now,

$$I = I_{SC} - I_o\left[e^{\left(\frac{q(V+IR_S)}{nKT}\right)} - 1\right] - \frac{V+IR_S}{R_P} \quad (1)$$

Where,

I: Solar cell current (A)

I_{SC}:Light generated current (A) [Short circuit value assuming no series/ shunt Resistance]

I_o: Diode saturation current (A);

q: Electron charge (1.6×10-19 C);

T: Cell temperature in Kelvin (K);

K: Boltzmann constant (1.38×10-23 J/K);

V: solar cell output voltage (V); R_S: Solar cell series resistance (Ω); R_P: Solar cell shunt (parallel) resistance (Ω)

n: is known as the "ideality factor" ("n" is sometimes denoted as "A") and takes the value between one and two [12].

3. Grid Connected PV System

3.1. Grid-connected or Utility-interactive Systems

Grid connected photovoltaic systems are the most common type as they make use of the existing main electricity grid. They are simpler in design and easier for the installers to fit than off grid systems [6].

-A grid-connected system is connected to a large independent grid (typically the public electricity grid) and feeds power into the grid.

-It is directly connected to the electricity network.

-Primary components are the inverter, or power-conditioning unit (PCU).

-No battery or other storage is needed.

-This is a form of decentralized electricity generation.

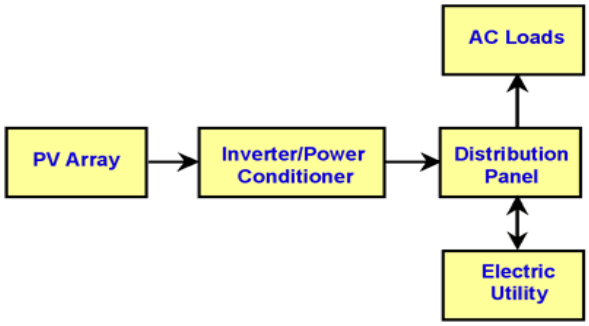

Fig. 2. The diagram of grid-connected photovoltaic system.

3.2. Stand-alone Systems or Off-grid Systems

This systems is particularly suitable in remote locations especially those where the property is more than one-quarter mile from the nearest power lines. Often the installation of an off grid PV system proves more cost-effective than extending the power lines [6].

-It is not linked to the mains electricity supply.

-It supplies electricity to a single system.

-It includes one or more batteries, which store the electricity.

-A charge controller is used to avoid battery damage and optimizing the production.

-But in direct coupled system no battery is needed.

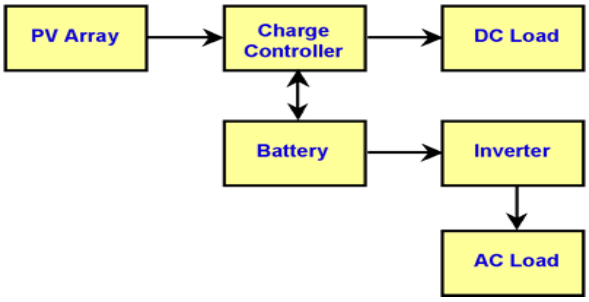

Fig. 3. The diagram of stand-alone PV system.

4. Load Sharing using SPWM Bridge Inverter

There are different methods of load sharing techniques using SPWM bridge inverter.

Droop control method and average power control method are the load sharing techniques developed in stand alone ac power system based on the power flow theory of an ac system [3],[4]. Another approach is the current injection method, a pll is deployed to monitor the zero crossing of the sytem voltage and the current is injected to the system to control the real and reactive power of the system.

4.1. Fundamental Building Block Diagram

A PV power inverter system in parallel with a load and utility grid is shown in Fig. 4. X_g Represents sum of synchronous reactance of generator and reactance of transmission line. The dc voltage obtained from PV array is converted to ac through the inverter. Transformer steps up the voltage. A LC filter is connected to remove unwanted harmonics. The power is then fed to the load.

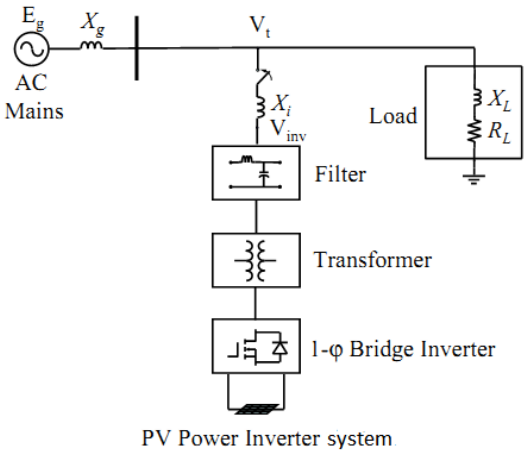

Fig. 4. Fundamental building block diagram of the grid connected PV system.

5. Principle of Load Sharing with Control of Real and Reactive Power

The load sharing principle in case of parallel-connected generators and grid connected PV system are described below separately.

5.1. In Parallel Connected Generators

Two parallel generators A and B shown in Fig 5. supply a load of a certain power and power factor. Controlling the mechanical power input and excitation respectively can control real and reactive power delivered from generators.

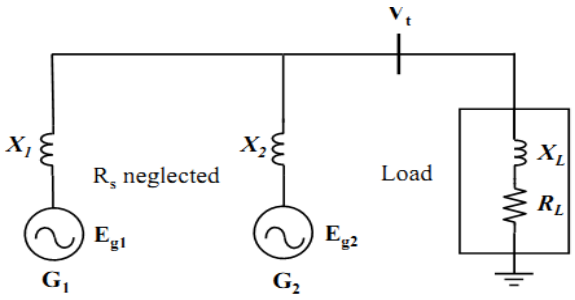

Fig. 5. Two parallel generators supplying a load.

5.1.1. Control by Changing Mechanical Power Input

The input mechanical power or shaft power to the generator can be changed by changing the opening of the valves through which steam (or water) enters a turbine. Real power delivered by generator is given by

$$P = \frac{E_g . V_t}{X} \sin \delta \qquad (2)$$

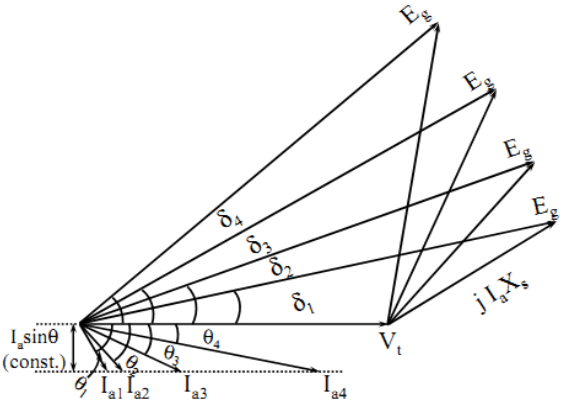

Fig. 6. Vector diagram of voltages and currents for change in shaft power input only in case of parallel generators.

If excitation I_f is kept constant, E_g will remain constant. Increasing the input shaft power will result the rotor speed start increasing. But rotor speed cannot exceed bus frequency. So δ will start to increase if V_t and X remain constant. The generator

will start delivering more real power. Again the real power delivered is

$$P = V_t . I_a . \cos\theta \quad (3)$$

From the vector diagram shown in Figure 7, we see that

$$E_g = V_t + jI_aX_s \quad (4)$$

If δ is increased keeping E_g constant, I_aX_s will increase. Since X_s is constant, I_a will increase. Again θ will decrease with the increase of δ. So $I_a \cos\theta$ will increase. Therefore, delivered real power $P = V_t . I_a . \cos\theta$ will increase. It is seen in the diagram that $I_a \sin\theta$ remains the same with the increase of δ. So the reactive power $Q = V_t . I_a . \sin\theta$ will remain constant.

5.1.2. Control by Changing Excitation

Let us reduce excitation I_f keeping the input shaft power constant. Since the input shaft power is constant, delivered real power will be constant. It implies that $E_g \sin\delta$ will remain constant. A reduction in I_f must reduce E_g. So $\sin\delta$ increases i.e. δ increases. Since V_t is considered constant, $I_a \cos\theta$ must remain constant for constant output real power. From the vector diagram shown in Fig. 7. it is seen that $I_a \sin\theta$ varies with the change of excitation.

So, the reactive power $Q = V_t . I_a . \sin\theta$ varies. Therefore it can be inferred that changing excitation only varies reactive power if input shaft power is kept constant.

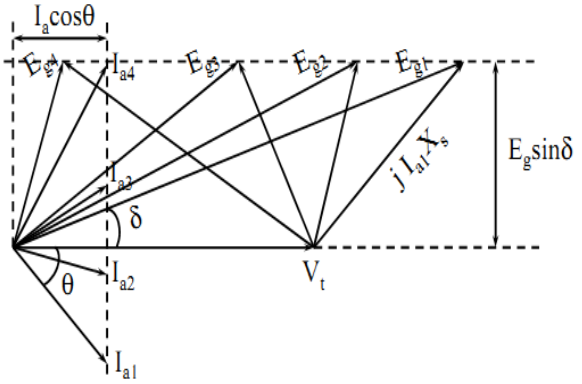

Fig. 7. Vector diagram of voltages and currents for change in excitation only in case of parallel generators.

5.2. In Grid-connected PV System

In the present grid-connected PV system scheme as shown in Fig. 8, power is fed to the load from the PV array. If the generation of power from PV array is not sufficient to serve the load demand, the deficit can be compensated from the grid. If the generated power is greater than the load demand, the excess power can be fed back to the grid.

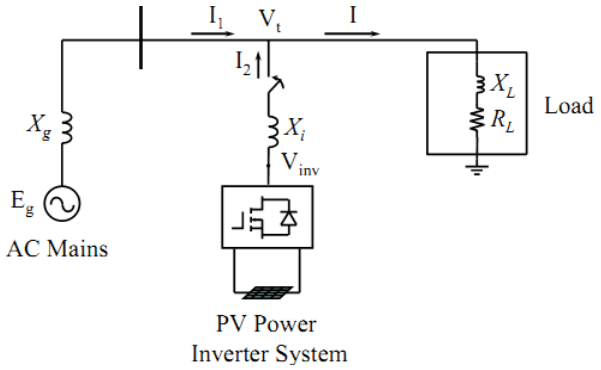

Fig. 8. Block diagram of the grid-connected PV system showing the sharing of load.

The vector diagram comprising the voltage and current vectors for the grid-connected PV system is shown in Fig. 9

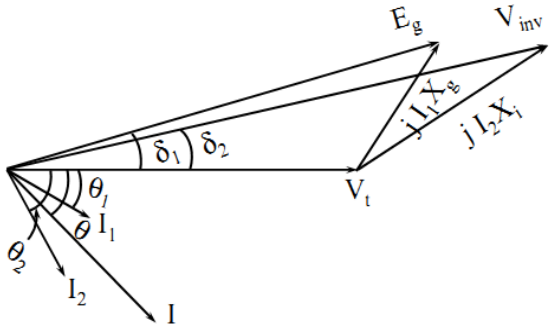

Fig. 9. Vector diagram for voltages and currents in grid-connected PV system.

5.3. Inverter Branch: Equivalent Circuit and Analysis for Voltages and Currents

The PWM voltage is fed to the transformer and its output is then filtered. The filtered voltage is fed to the grid through an inductance X_i. The grid voltage is V_t whose variation must be within a specified range.

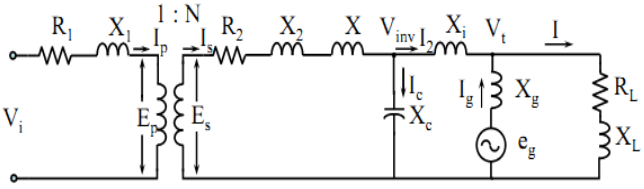

Fig. 10. Equivalent circuit of the grid-connected PV system.

The transformer shown in Fig. 10 are expressed by its equivalent circuit. If all the parameters on the primary side are referred to the secondary then the above circuit takes the form shown in Fig. 11

Here, $R_{eq} = R_1N^2 + R_2$; $X_{eq} = X_1N^2 + X_2 + X$

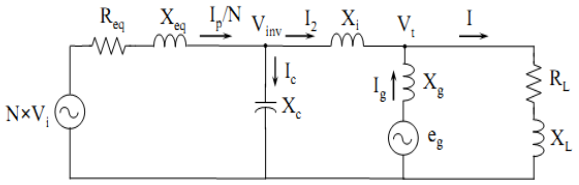

Fig. 11. Primary parameters of inverter branch of Fig. 10 referred to secondary.

6. Formation of Equation for Voltages and Currents Draw their Vector Diagrams and Wave Shapes

Applying superposition theorem in the circuit shown in Fig. 11, the equation for I_2, I_g and I can be developed.

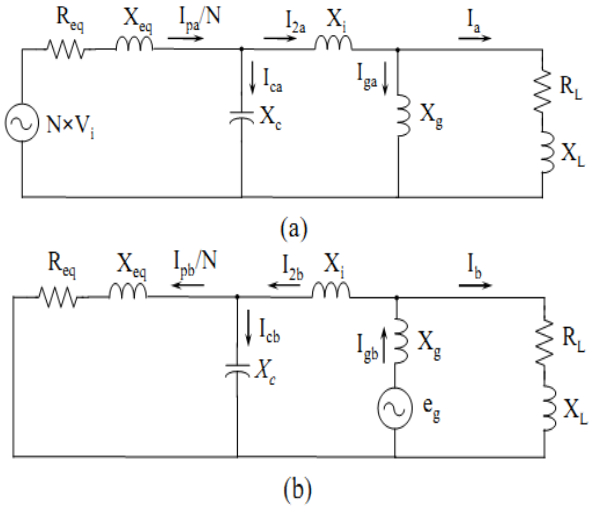

Fig. 12. Applying superposition theorem in the circuit of Fig. 11, (a). When $N \times V_i$ present only (b). When e_g present only.

From fig. 12(a),

$$\frac{I_{pa}}{N} = \frac{N \times V_i}{Z_{eq} + (-jX_c) \| (jX_i + Z_a)}$$

$$Z_a = (jX_g) \| (R_L + jX_L)$$

$$I_{2a} = \frac{I_{pa}}{N} \times \frac{-jX_c}{(-jX_c + jX_i + Z_a)}$$

$$I_{ga} = I_{2a} \times \frac{(R_L + jX_L)}{(R_L + jX_L + jX_g)}$$

$$I_a = I_{2a} - I_{ga}$$

From fig. 12(b),

$$I_{gb} = \frac{e_g}{(R_L + jX_L) \| (Z_{aa} + jX_i) + jX_g}$$

Where, $Z_{aa} = (-jX_c) \| (R_{eq} + jX_{eq})$

$$I_{2b} = I_{gb} \times \frac{(R_L + jX_L)}{(R_L + jX_L + Z_{aa} + jX_i)}$$

$$I_b = I_{gb} - I_{2b}$$

$$I_2 = I_{2a} - I_{2b}; I_{g=}I_{gb} - I_{ga}; I = I_a + I_b$$

7. The Proposed Model

In our reasearch we have proposed a SPWM boost DC to AC converter followed by a Static Var Compensator (SVC) to control the reactive power from the PV panel. More over to regulate the real power we have adjusted the modulation index of the SPWM inverter. The topology is presented below.

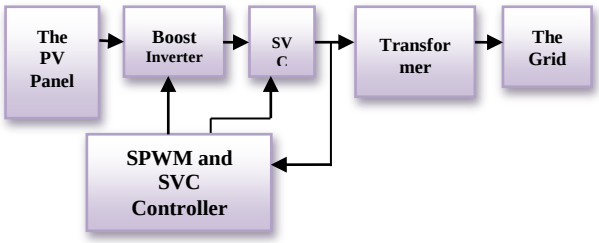

Fig.13. The proposed model.

7.1. The SPWM Boost Inverter

By briefly studying the behavior of the Boost Inverter on grid connected PV system; several significant features have been found which are mentioned below:

- More silicon less iron and compact size
- Reduction of transformer size.
- Elimination of harmonics and power savings is high
- No filter is needed and cost effective and.
- No MPPT charge controller is needed.

7.2. Static Var Compensator(SVC)

We have used a variable shunt capacitor as the SVC in our proposed system.The power factor correction can also be illustrated from power triangle.

Thus referring to Fig. 14, the power triangle *OAB* is for power factor $\cos\Phi_1$, whereas power triangle *OAC* is for the improved power factor $\cos\Phi_2$.

It may be seen that active power (OA) does not change with power factor improvement. However, the lagging KVAR of the load is reduced by the p.f. correction equipment, thus improving the p.f. to $\cos\Phi_2$. Leading KVAR supplied by p.f. correction equipment

$= BC = AB - AC$

$=KVAR1 - KVAR2$

$= OA(\tan\Phi_1 - \tan\Phi_2)$

$$= KW\ (\tan \Phi_1 - \tan \Phi_2) \quad (5)$$

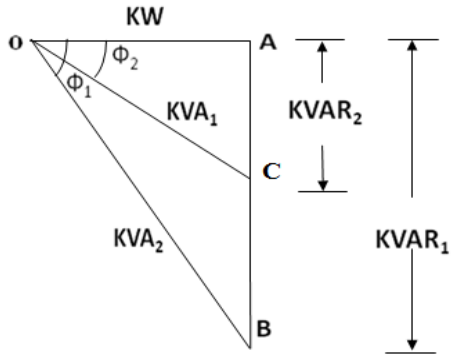

Fig. 14. The power triangle.

Knowing the leading KVAR supplied by the p.f. correction equipment, the desired results can be obtained. It can be shown that, the reactive power supplied by the Capacitor

$$= V_c I_c \quad (6)$$

Where, $I_c = \frac{V_c}{X_c}$ *and* $X_c = \frac{1}{2\pi fc}$

From equation (5) and (6)we can show that

$$C = \frac{2\pi f.KW\ (\tan \Phi_1 - \tan \Phi_2)}{V_c^2} \quad (7)$$

Using the equation (7) we can easily calculate the value of C from known values of f, KW, Φ_1, Φ_2 and V_c. We have used this relation to compensate reactive power supply from our inverter.The transformer used in the next stage is a low frequency step up transformer with a low turns ration. The use of boost inverter substantially reduced the size of the transformer, so as the cost. It meets our one of the objective of design using less iron and more siicon.The design can be realized without the transformer also but we have intentionally used the transformer to get a safe isolation at the user premises.

8. Details Circuit Configuration and Simulations Results

By thoroughly analyzing the aforementioned circuit diagram for several voltage levels and by varying the modulation indices for each of these different voltages the following set of data can be found.

V_{in} =24v (DC)
For Modulation index=0.50 (Without capacitance C5)
V_1=12;
V_2=−12;
TR=0.248ms;
TF=0.001ms;
PW=0.001ms;
TD=0;
$V_{ampl} = 6.0$ V;
Frequency=50Hz;
$C_3 = C_4 = 250\mu f$;
$L_3 = L_4 = 7.8$ mh;
$R_{load} = 200\Omega$;
L_{load}=0.1h

8.1. *The Circuit Diagram*

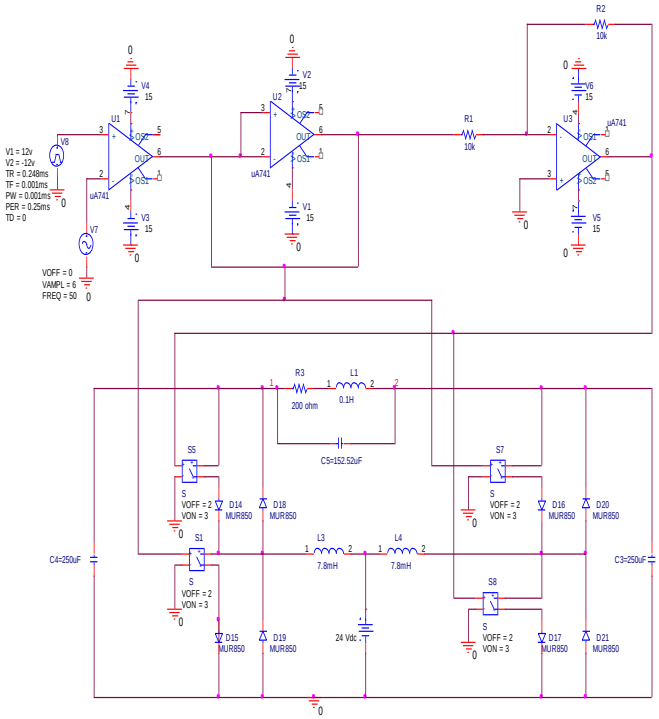

Fig. 15. The Detailed Circuit Configuration.

8.2. *Output Curves*

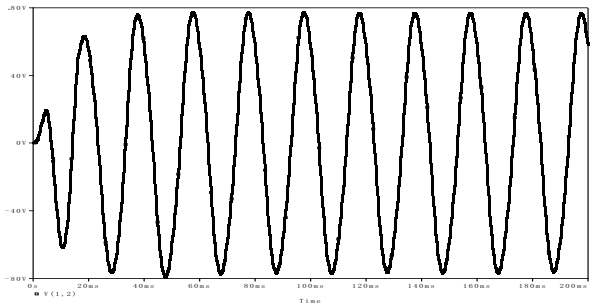

Fig. 16. Output voltage (V_{out}) without capacitance (C_5).

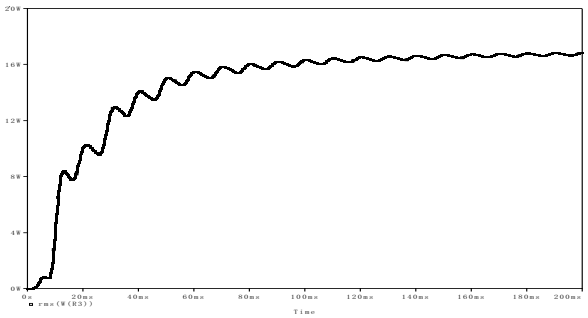

Fig. 17. Output real power (P_{rms}) without capacitance (C_5).

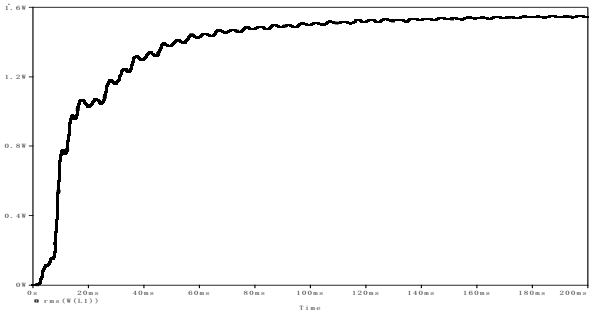

Fig. 18. Output reactive power (Q_{rms}) without capacitance (C_5).

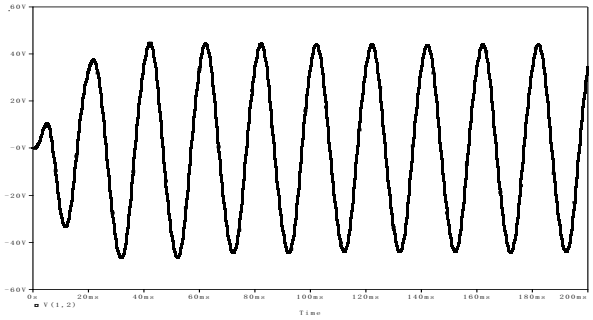

Fig. 19. Output Voltage (V_{out}) with capacitance (C_5=152.50μF).

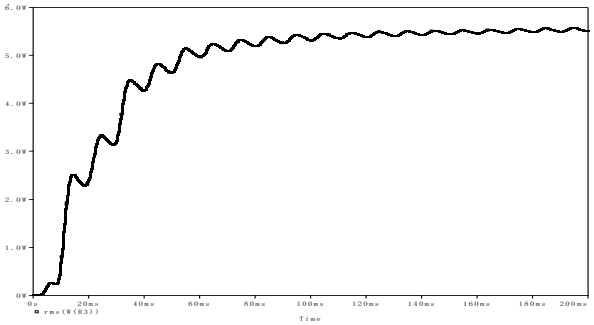

Fig. 20. Output real power (P_{rms}) with capacitance (C_5=152.50μF).

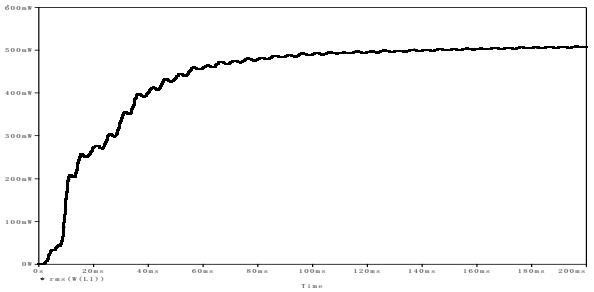

Fig. 21. Output reactive power (Q_{rms}) with capacitance (C_5=152.50μF).

8.3. Data Tables

Table 1. Data for the variation of different modulation index for input 24V (DC).

Modulation index	$V_{amplitude}$ (v)	Output voltage, V_{out}(v)	Real power, P_{rms}(w)	Reactive power, Q_{rms}(var)	%THD	Value of capacitance,C_5 (μf)
0.333	4.0	43.82	5.63	0. 51	1.58	20
0.375	4.5	44.50	5.61	0. 51	0.45	70
0.416	5.0	45.13	5.66	0. 51	1.03	95.55
0.458	5.5	44.16	5.47	0. 51	1.53	123.50
0.500	6.0	44.52	5.57	0. 51	2.41	152.50
0.542	6.5	44.30	5.54	0. 51	3.40	181.85
0.583	7.0	43.72	5.47	0. 51	4.59	215.35

Table 2. Control of reactive power by applying parallel compensation (capacitance C_5) by keeping it at a constant value of 0.51 var.

Modulation index	$V_{amplitude}$ (v)	Output voltage, V_{out}(v)	Real power, P_{rms}(w)	Reactive power, Q_{rms}(var)	% of total harmonic distortion(%THD)
0.333	4.0	42.21	5.48	0.50	2.28
0.375	4.5	49.90	7.63	0.70	2.11
0.416	5.0	58.10	10.05	0.92	2.48
0.458	5.5	67.09	13.06	1.20	2.78
0.500	6.0	76.66	16.90	1.56	3.42
0.542	6.5	81.17	19.44	1.77	4.36
0.583	7.0	81.29	20.62	1.81	6.25

In a power system of conventional parallel-connected generators, share of real power and reactive var of an incoming generator are controlled by differnet ways like adjusting shaft power input and field excitation. The circumstances of load sharing by a grid connected PV system is however different. There is no prime mover or excitation source are present in PV system. Sometimes in case of power crisis, there is a need for the transfer of PV power to the grid systems. In that case the

real and reactive power for load sharing in grid connected PV power system can be easily controlled as well as changed by changing the modulation index of the boost inverter. By our proposed model we can easily control the real and reactive power efficiently by using an inverter and SVC feedback system.

9. Conclusion

After analyzing the overall research we can finally predict that without the SVC feedback the output voltage of the boost inverter has increased with the increase of the modulation index (m_a). The real power, reactive var and the percentage of total harmonic distortion (%THD) has also followed the similar pattern. However, in case of the SVC feedback while keeping the reactive var constant; the output voltage, real power and the percentage of THD did not follow any predictive pattern. In addition to this, they were bounded within a particular range with the increase of the modulation index. Moreover, no significant fluctuation has been marked in the entire set of data for the SVC feedback. Finally we can recapitulate that, for a fixed load power factor, the real and reactive power can be varied by changing the modulation index (m_a), the output voltage of the boost inverter can also be varied and the total harmonic distortion (%THD) has also varied in a predictive manner. So our future plan is to develop a mathematical model for the robust controlling of boost inverter's output voltage & power. The real power will be varied while the reactive power would be kept constant and vice versa. In doing so, the THD should be kept low to maintain a high efficiency.

References

[1] Control Strategy for Load Sharing in Grid-Connected PV Power System", ICECE, Dhaka, Bangladesh, 2008.

[2] R. Akhter, "A new technique of PWM Boost inverter for solar home application", BRAC University Journal, Vol. IV, No. 1, 2007.

[3] A. A. S. Khan, K. M. Rahman, "Voltage Mode Control of Single Phase Boost Inverter", 5th International Conference on Electrical and Computer Engineering ICECE 2008, 20-22 December 2008, Dhaka, Bangladesh.

[4] C. Cecati, A. D. Aquila and M. Liserre, "Analysis and control of a three-phase dc/ac step-up converter", in proc. IEEE ISIE'02 Conf. paper. 850-856, July 2002.

[5] Photovoltaic Panel Simulation User's Guide, Educational Bookmarks, Australian Cooperative Research Centre for Renewable Energy (ACRE), August 14—1998.

[6] C. J. Hatiziadoniu, F. Chalkiadakis, and V. Feiste, ''A power conditioner for a grid-connected photovoltaic generator based on the 3-level inverter,'' IEEE Trans. Energy Conv., vol. 14, no. 4, pp. 1605--1610, Dec. 1999.

[7] K. Y. Khouzam, ''Technical and economic assessment of utility interactive PV systems for domestic applications in South East Queensland,'' IEEE Trans. Energy Conv., vol. 14, no. 4, pp. 1544-1550, Dec. 1999.

[8] M.C. Chandorkar, M.D. Divan, R. Adapa, "Control of parallel connected inverters in standalone ac supply systems," IEEE Transactions on Industry Applications, Vol. 29 No 1, 1993, pp. 136 –143.

[9] A. Tuladhar, H. Jin, T. Unger, and K. Mauch, "Control of parallel inverters in distributed ac power systems with consideration of line impedance effect," IEEE Trans. Ind. Applicant., vol. 36, pp. 131–138, Jan./Feb. 2000.

[10] Marwali, M.N. Jin-Woo Jung Keyhani, "A. Control of distributed generation systems - Part II: Load sharing control," IEEE Tran., Power Electron., Vol. 19, Issue. 6, pp. 1551-1561. Nov. 2004.

[11] Wu, T.-F., Shen, C.-L., Chang, C.-H. Chang, and Chiu, J.-Y., 2003a, "A 1ϕ3W Grid-Connection PV Power Inverter with Partial Active Power Filter," IEEE Transactions on Aerospace and Electronic Systems ,Vol. 39, No. 2, pp. 635-646, 2003

[12] Vikrant.A.Chaudhari, "Automatic Peak Power Traker for Solar PV Modules Using dSpacer Software." in Maulana Azad National Institute Of Technology vol. Degree of Master of Technology In Energy. Bhopal: Deemed University, 2005, pp. 98.

[13] M. Azab, "A New Maximum Power Point Tracking for Photovoltaic Systems," in WASET.ORG, vol. 34, 2008, pp. 571-574.